Spectroscopies vibrationnelles et d'absorption utilisant source laser et rayonnement synchrotron: synergie entre Raman, Infrarouge et Fluorescence

Paul Dumas [1,2]

1-Synchrotron SOLEIL (Gif sur Yvette)
2-CEA-DAM (Bruyeres Le Chatel)

Raman, Infrarouge et Fluorescence: Les processus

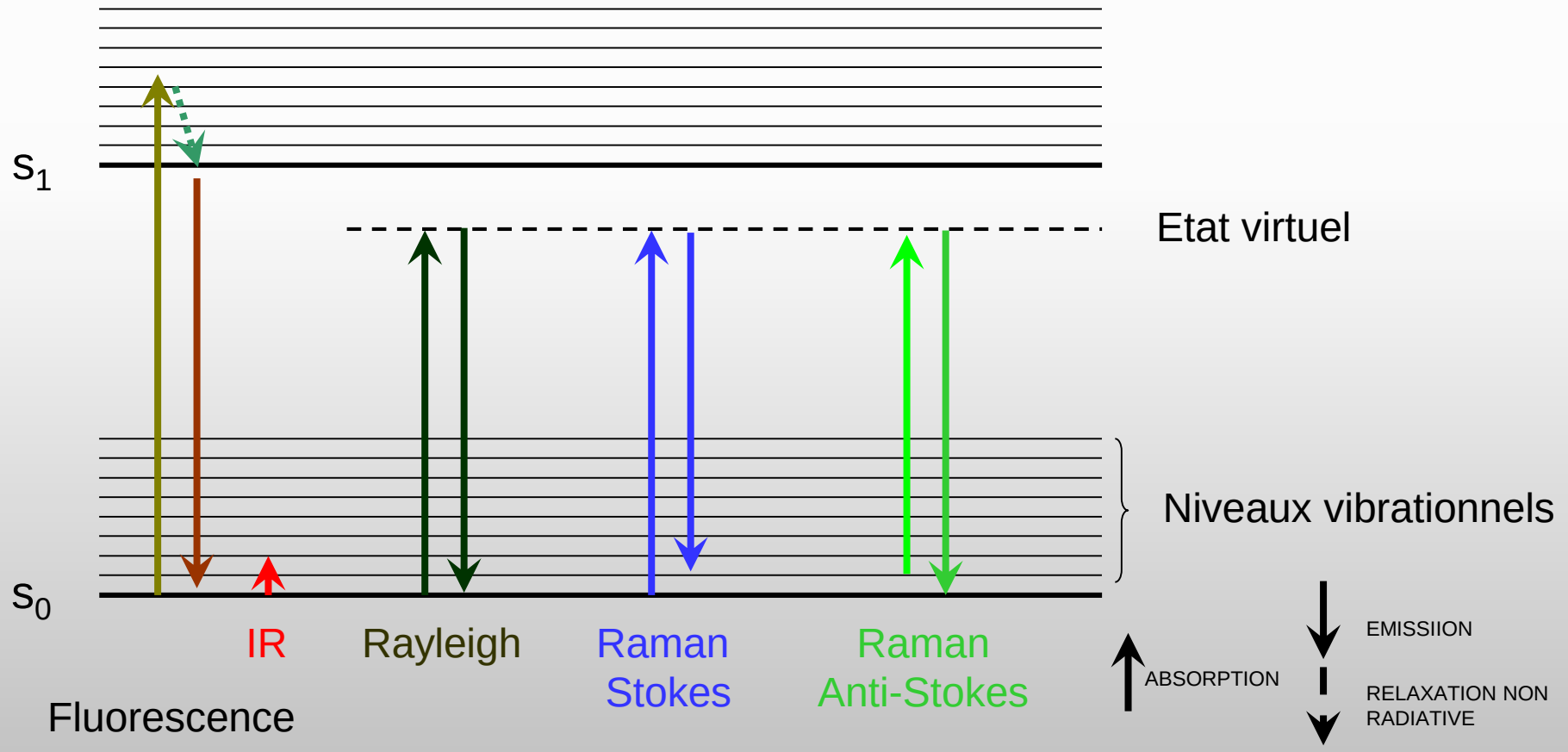

Spectroscopie vibrationnelle

La spectroscopie infrarouge nécessite de faire interagir un rayonnement dans l'infrarouge avec les molécules et de détecter les longueurs d'onde qui ont perdu de l'intensité (absorbées!)

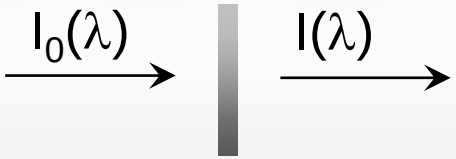

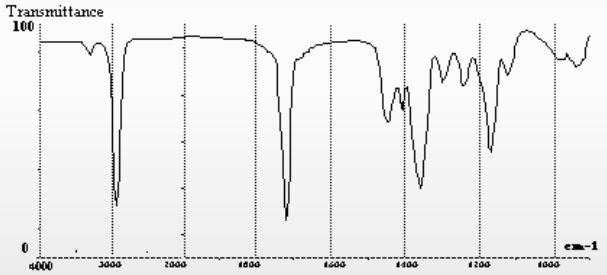

La spectroscopie Raman utilise un faisceau excitateur à une fréquence bien précise (laser en général) et recueille les émissions issues des processus d'interaction inélastiques

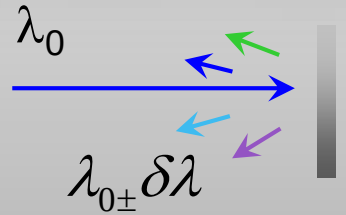

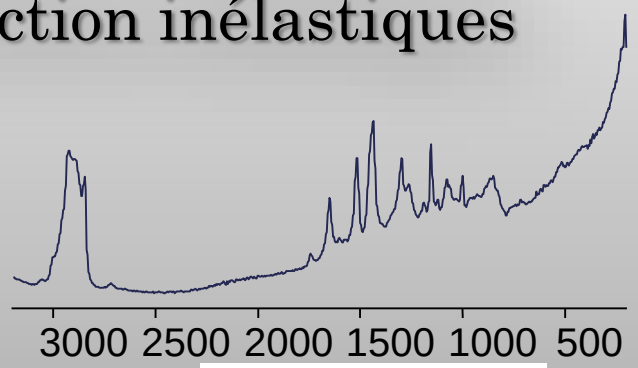

Spectroscopie de fluorescence

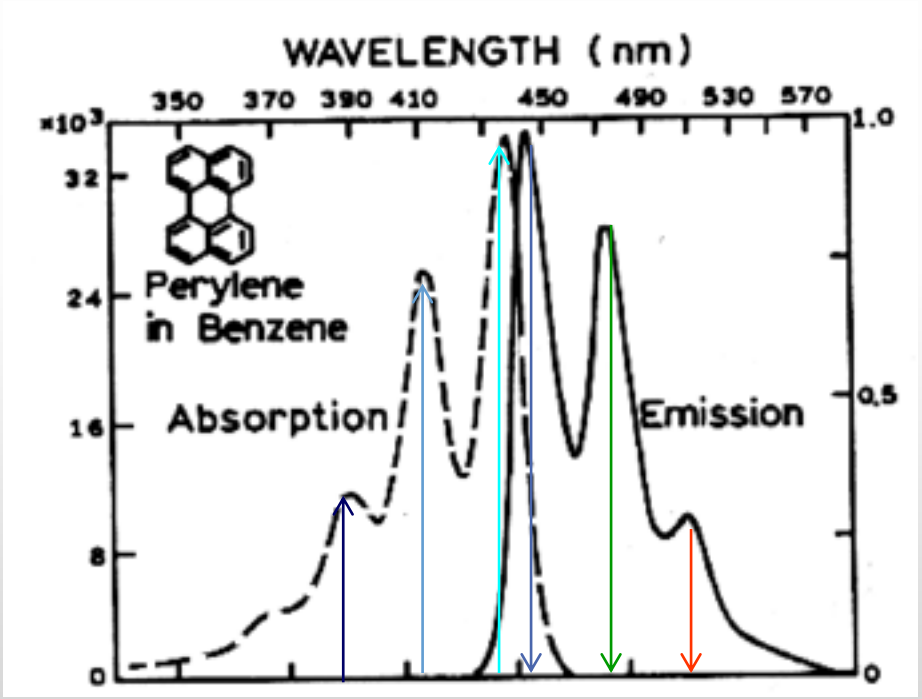

Energie

Energie

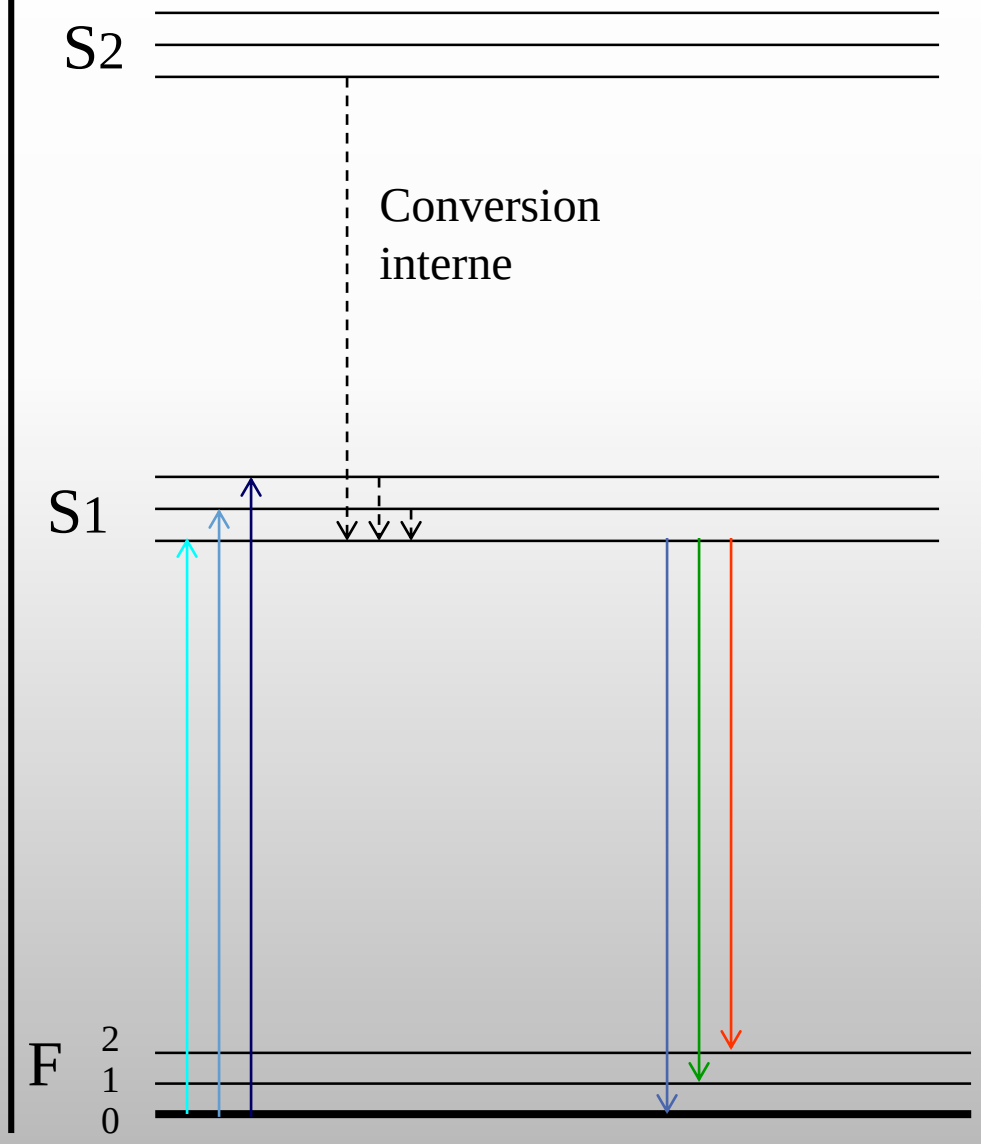

Spectre de fluorescence necessite des déconvolutions, des references

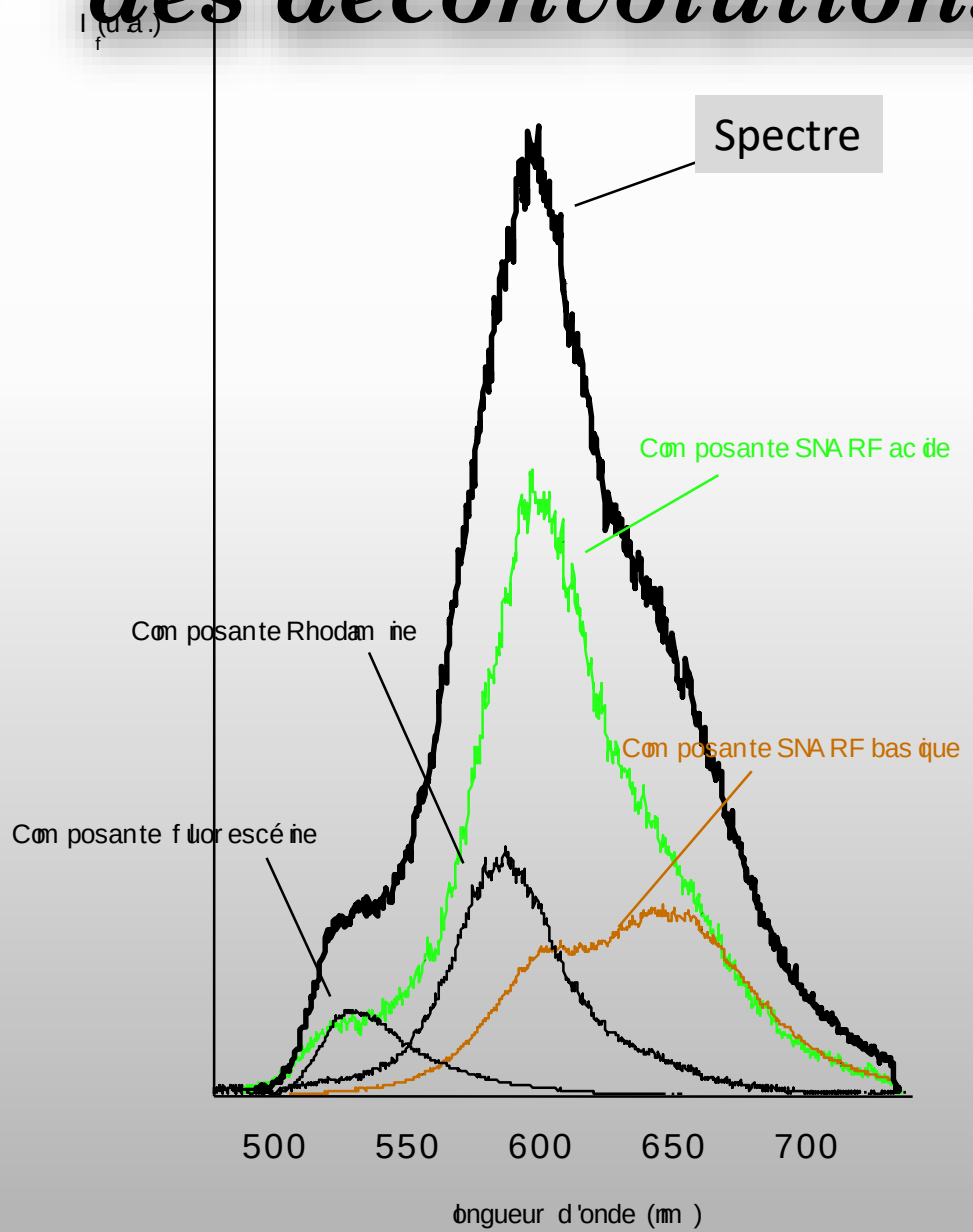

On utilise des spectres modèles pour chaque composante

Règles de sélection en spectroscopie vibrationnelle : complémentarité

Infrarouge: <u>Variation du moment dipolaire dynamique</u>

$$(\delta\mu / \delta q)_0 \neq 0$$

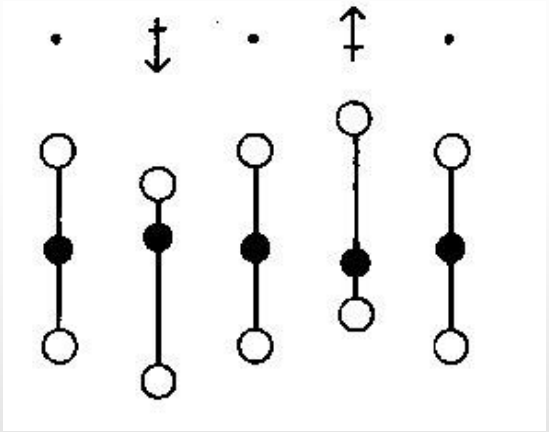

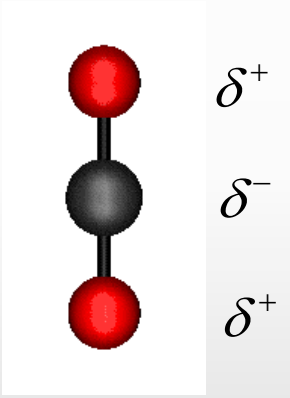

Raman : <u>Variation de la polarisabilité de la molécule</u>

$$P = \alpha E$$

$$(\delta\alpha / \delta q)_0 \neq 0$$

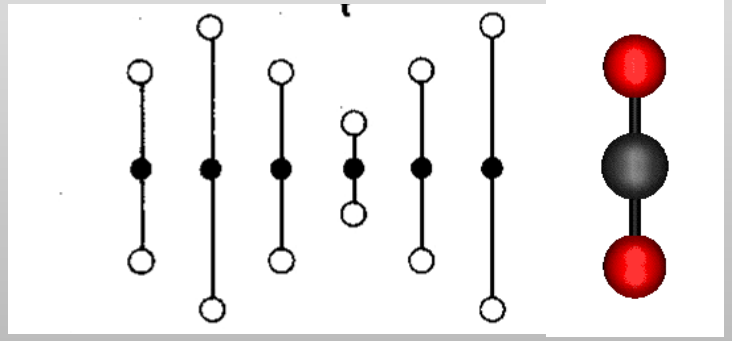

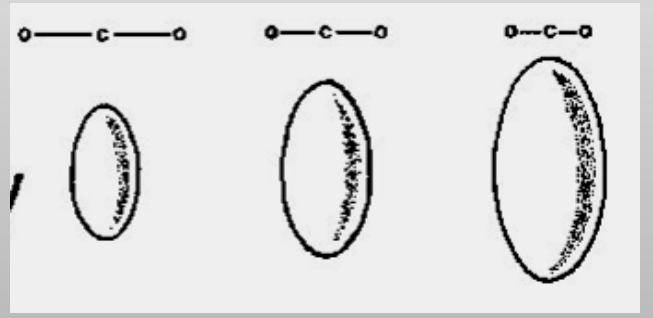

Complémentarité pour analyse approfondie

Spectre de l'acétate de méthyle

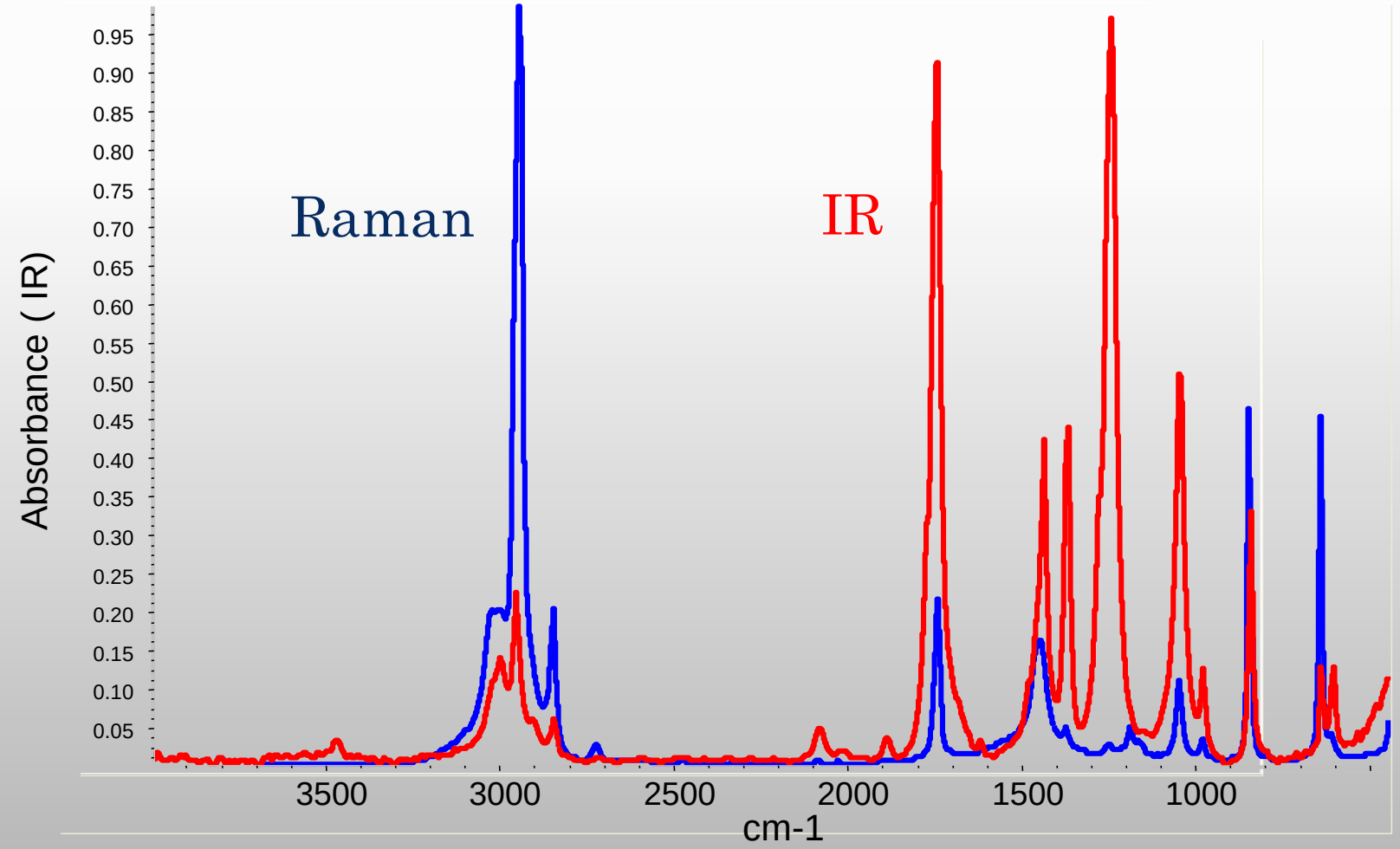

Instrumentation ,microscopie et source de photons

Spectromètre IR et Raman

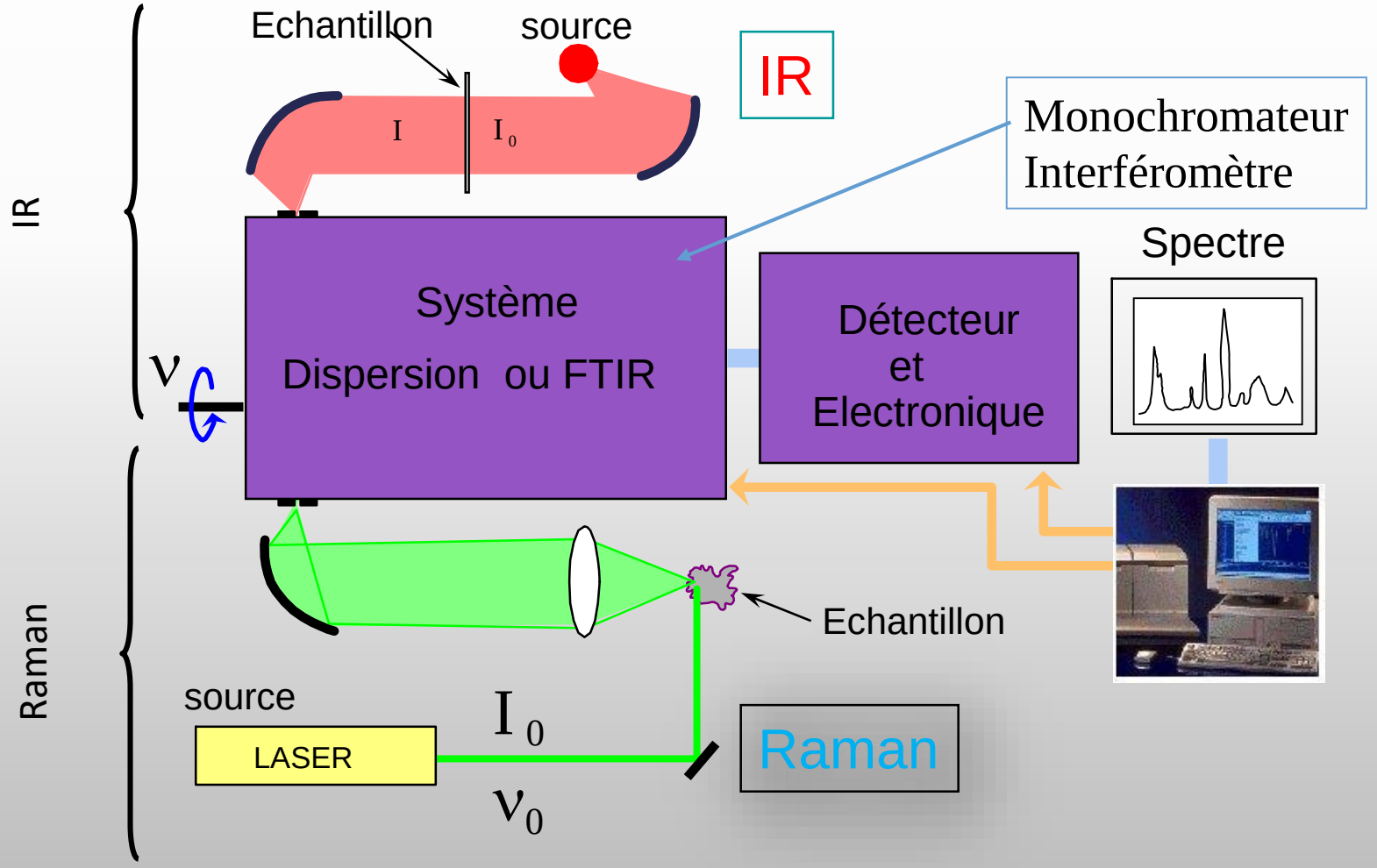

A l'intérieur d'un spectromètre Infrarouge

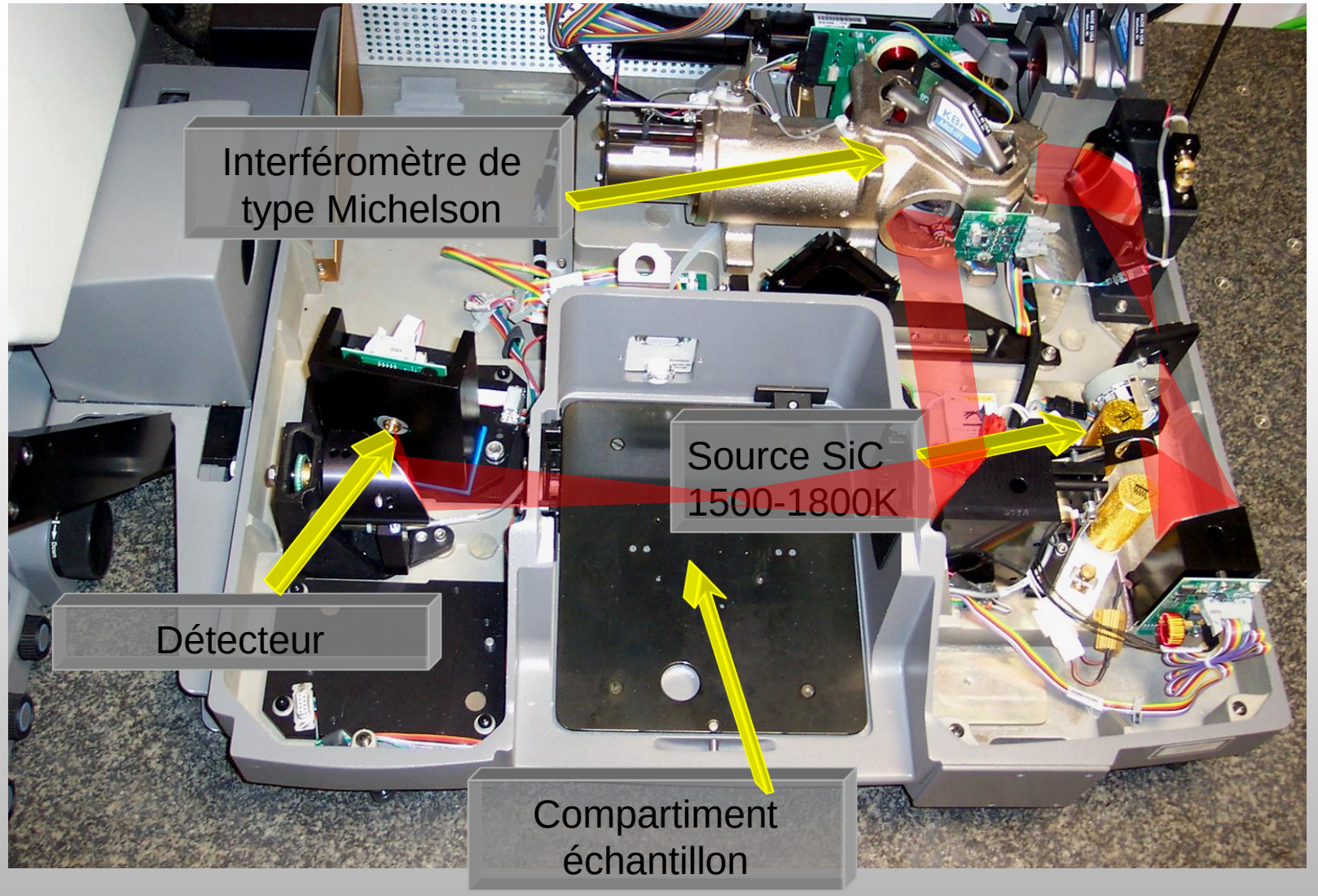

Couplage avec un microscope

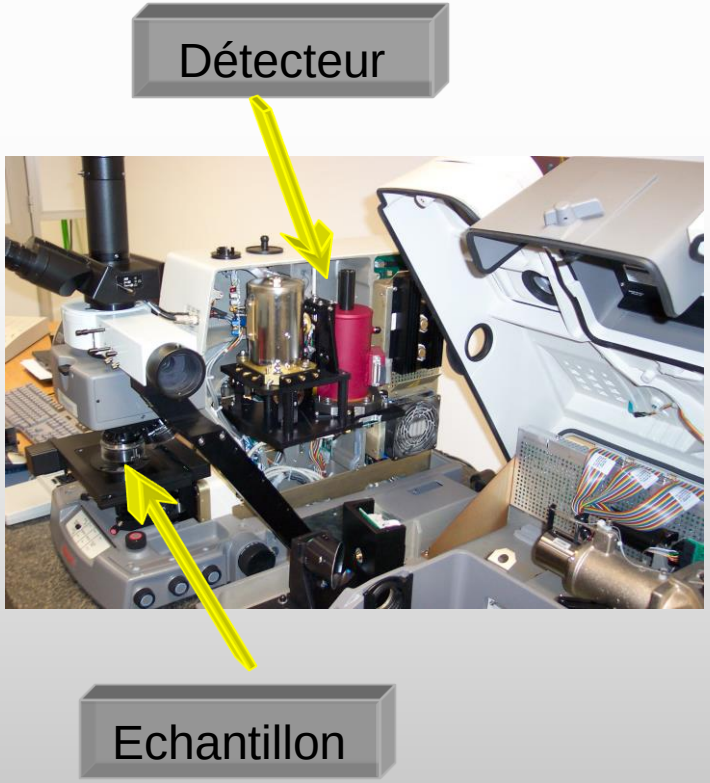

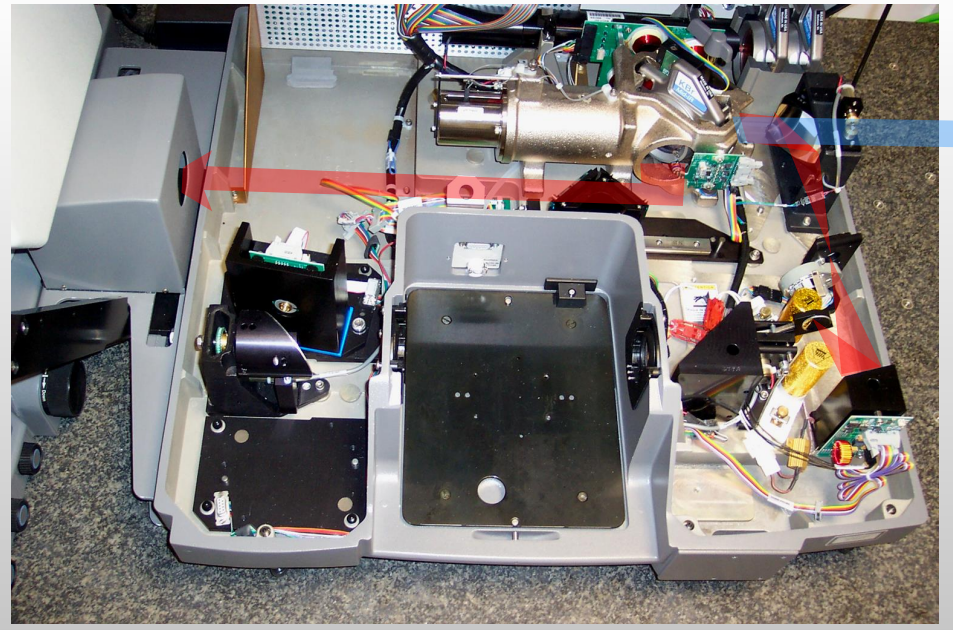

Interferogramme et avantage de Folgett

C'est ce qu'enregistre le détecteur

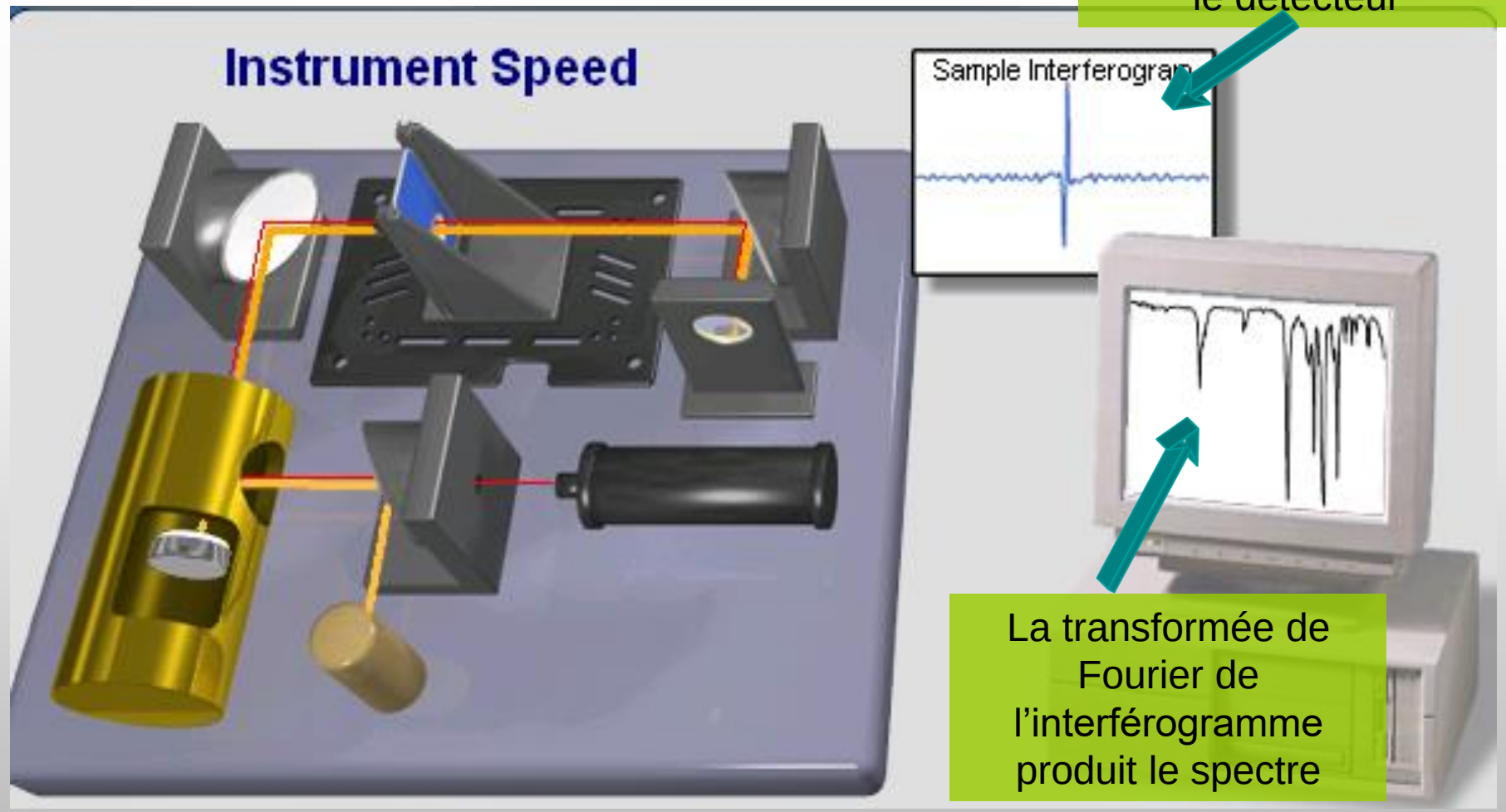

La transformée de Fourier de l'interférogramme produit le spectre

Premier exemple de couplage: Infrarouge et fluorescence

Analyse complémentaire en fluorescence

Lampe mercure

Coin cubes analyses

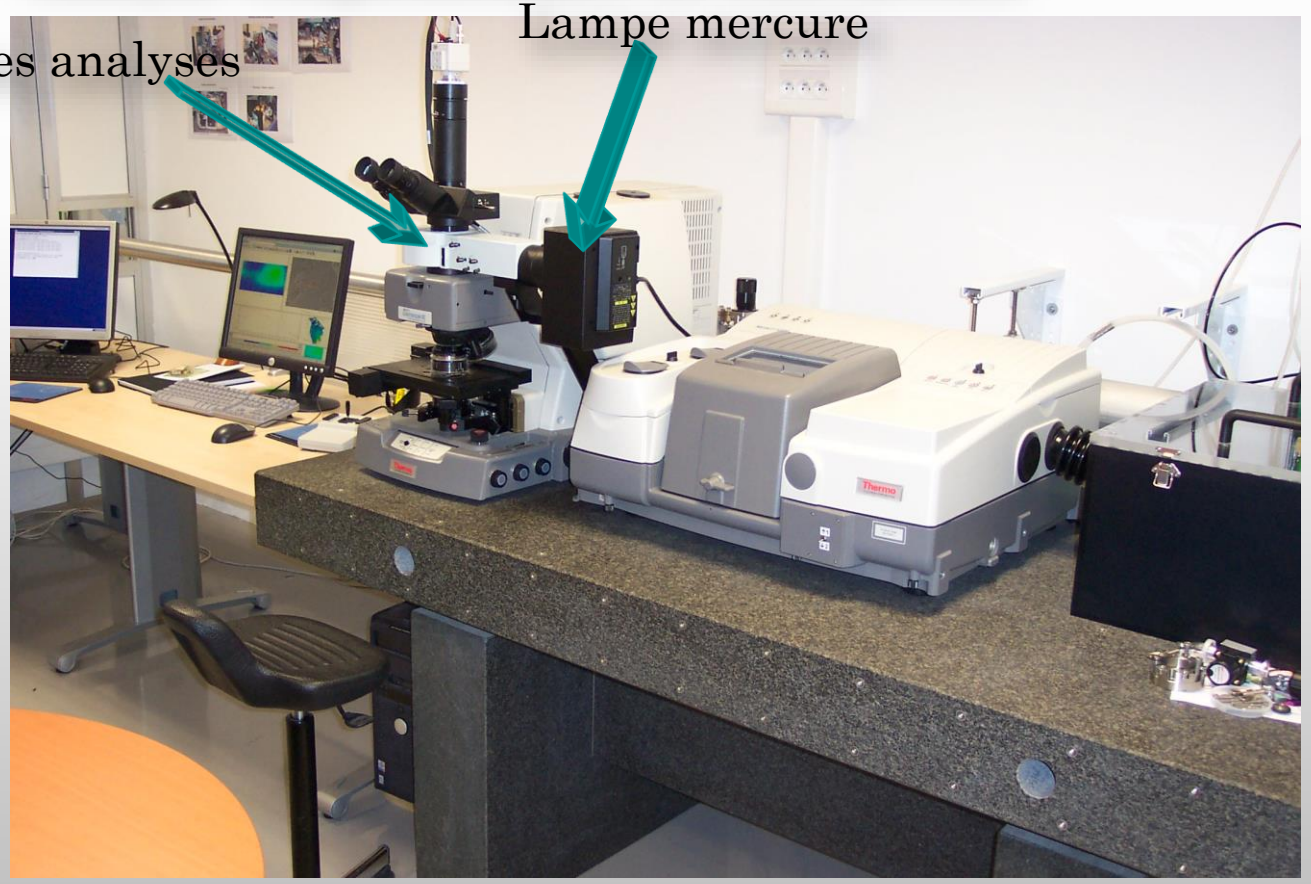

Spectrométrie Raman en mode dispersif

Discrimination importante, tout en gardant en mémoire que l'effet Raman est faible

PMT
DAD
CCD

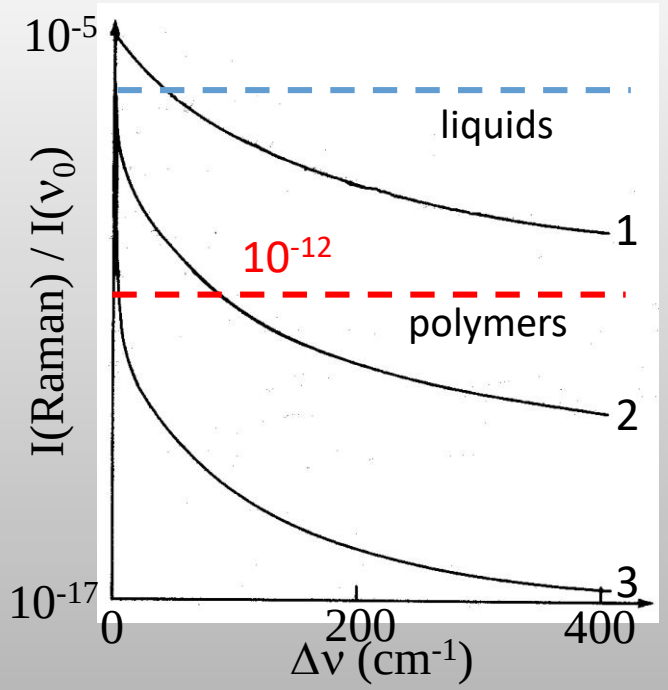

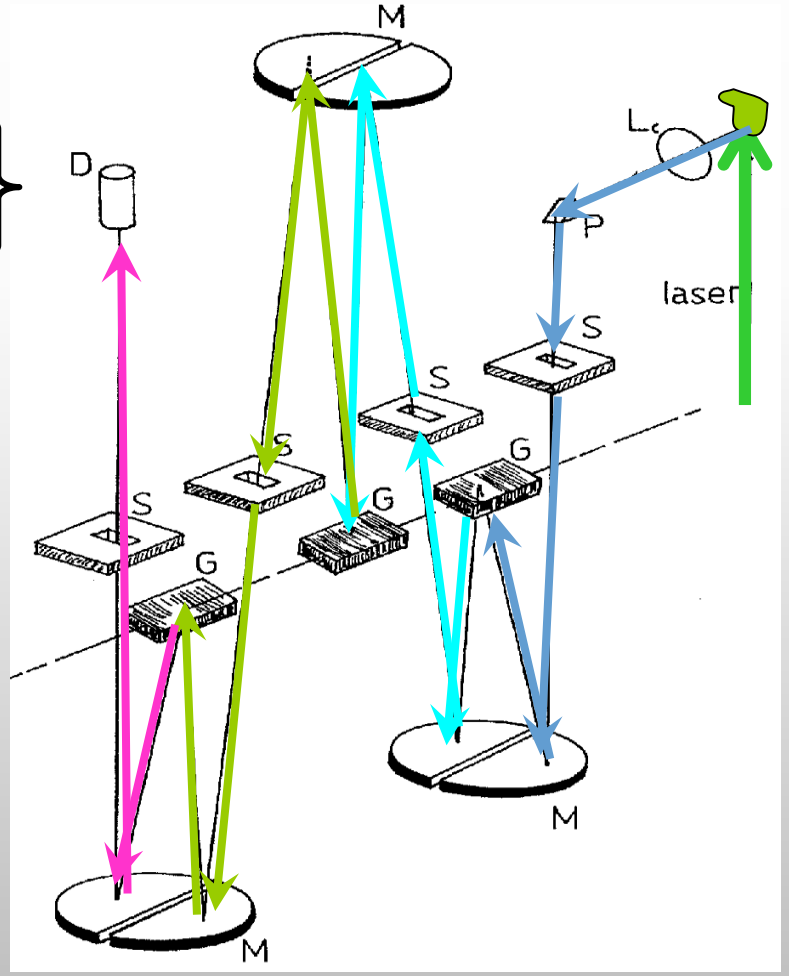

He-Ne (red)
Ar^+ (green)
Ti-Za (tuneable)

Triple monochromateur

Microscope Raman

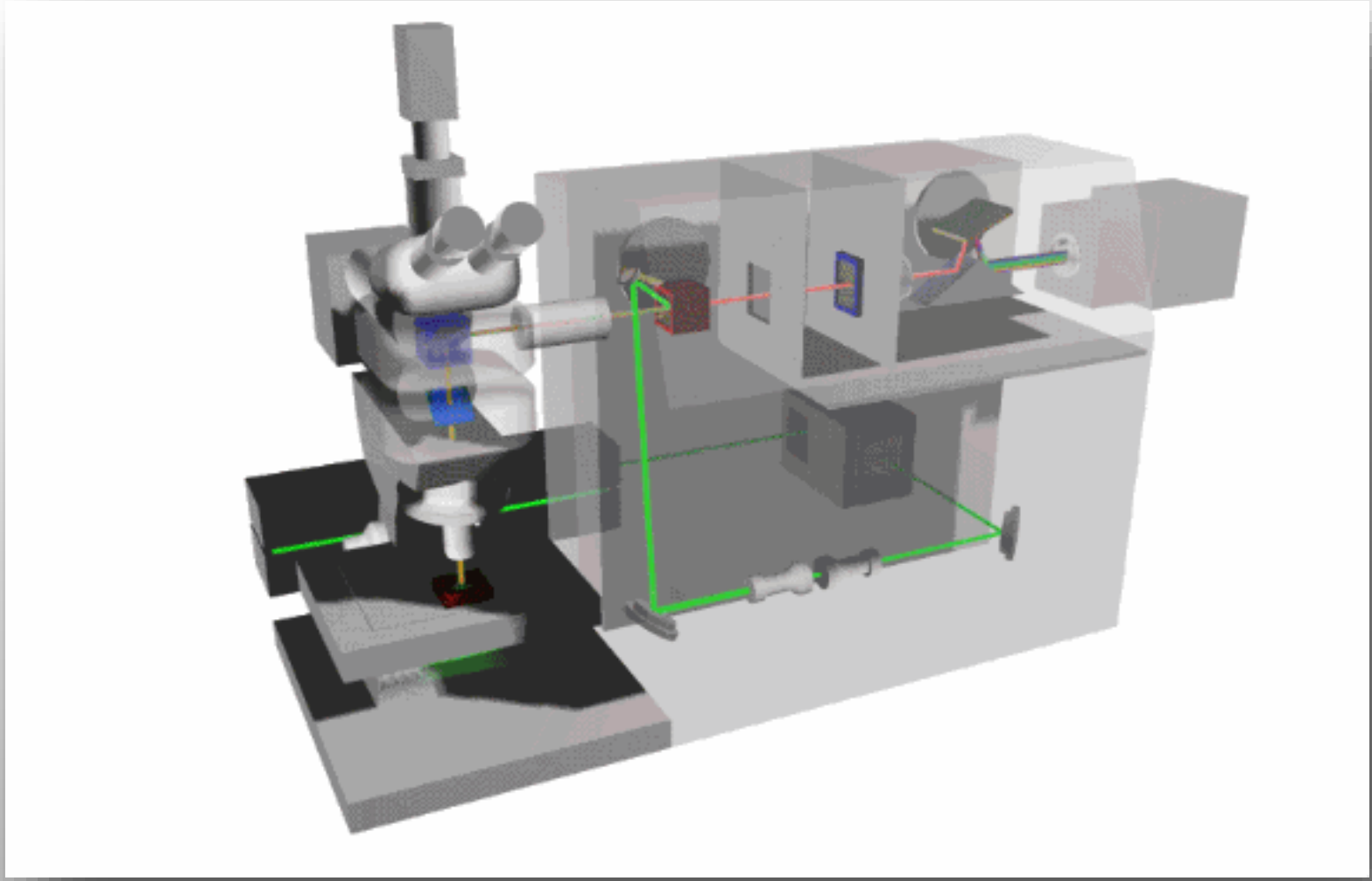

Infrarouge? Raman? Que choisir?

	IR	Raman
Echantillon	A peu près tous sauf solutions aqueuses	Tout type d'échantillon:; films, poudre, fibres, solutions, etc.
Préparation des échantillons	Préparation obligatoire pour presque tous (microtome, polissage)	Pas de prération spéciale
Taille des échantillons	Limité en épaisseur (< 10 μm transmission))	Toute taille
Cellules	Matériaux spéciaux, avec les inconvénients suivants :toxique, fragile, hygroscopique, cout)	Le verre est idéal
Purge	Necessaraire	Pas nécessaire
Solvents	Limités. Eau pratiquement impossible	Toute sorte, même l'eau
Temperature	Facile	Facile
Détection des traces (limite détection)	Grande	Plus faible
Microscopie	Limité par la diffraction avec le synchrotron	~1 μm
Limitations	Solutions aqueuses	Couleur, fluorescence
Qualité des spectres	****	**

Microscope de Fluorescence

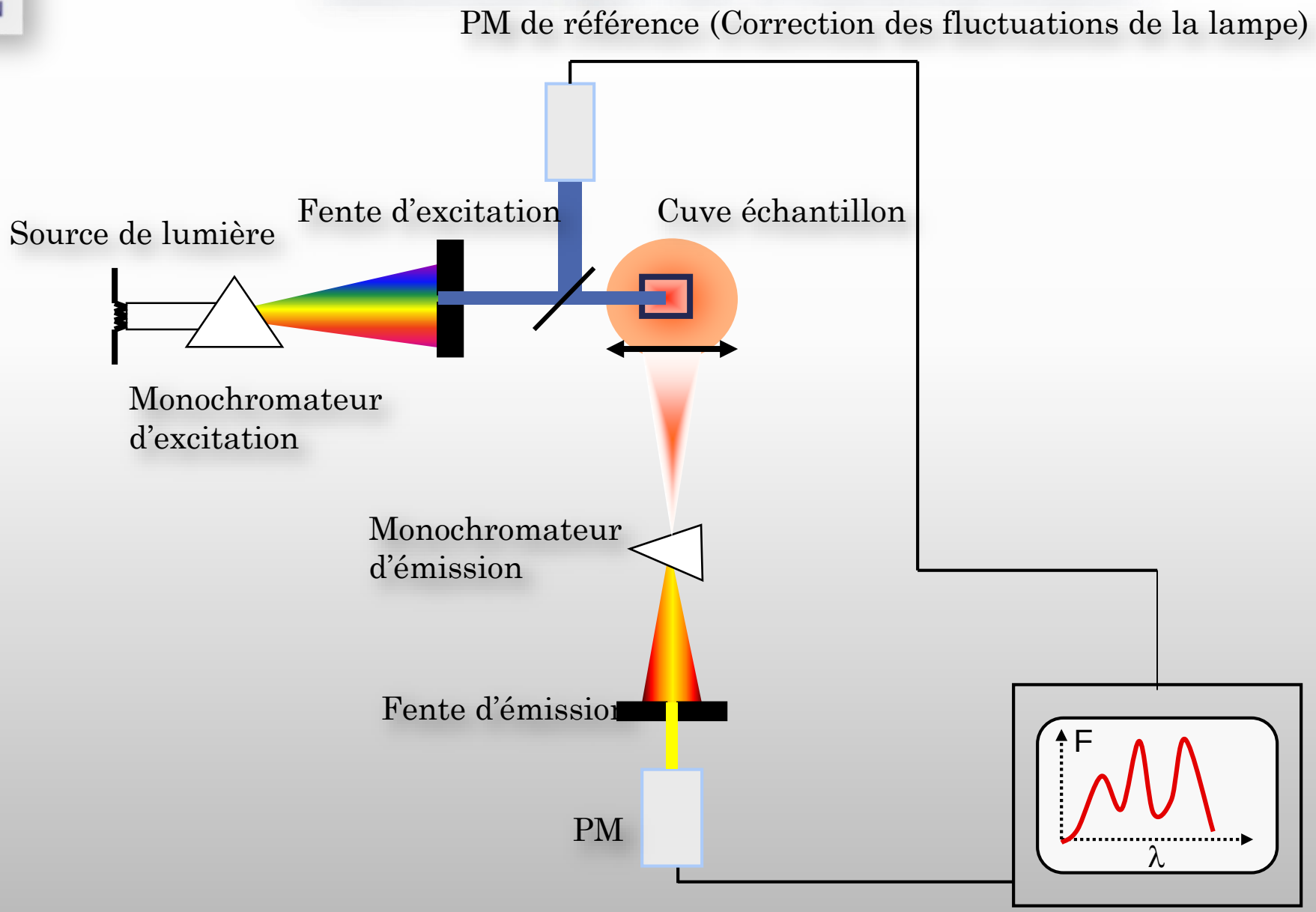

Microscope de Fluorescence

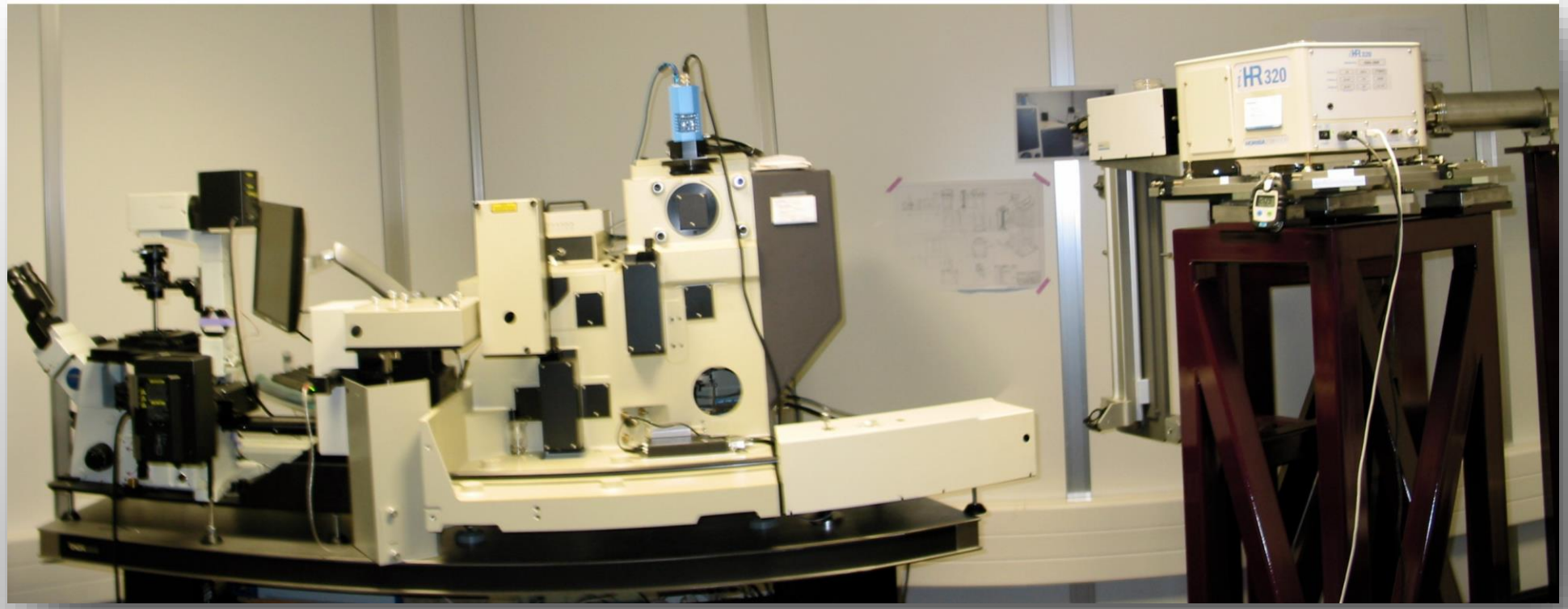

Ligne de lumière DISCO @ SOLEIL

Imagerie IR, Raman et de Fluorescence
Exemples et complémentarité

Nature des inclusions et identifications de l'environnement

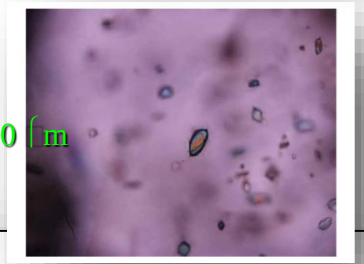

4000 to 7000 ppm wt H20
in cpx and opx, nothing garnet

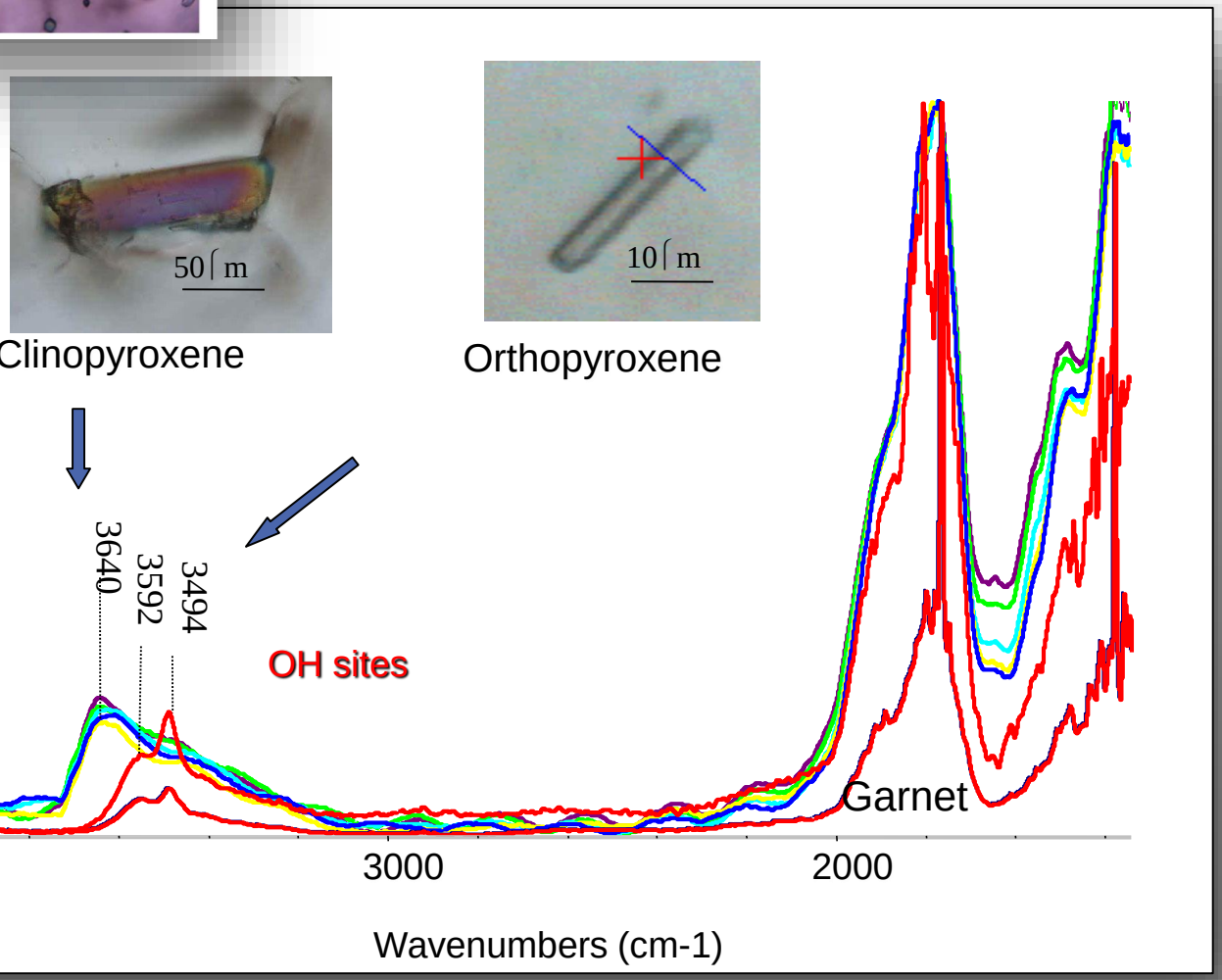

N. Guilhaumou, P. Dumas Oil & Gas Science and Technology - Rev. IFP, Vol. 60 (2005), No. 5, pp. 763-779

IR spectra of phases in garnet lherzolite: Example from Thaba Putsoa

Hcpx > Hopx>> Holiv >> Hgnt (Hsp = 0)

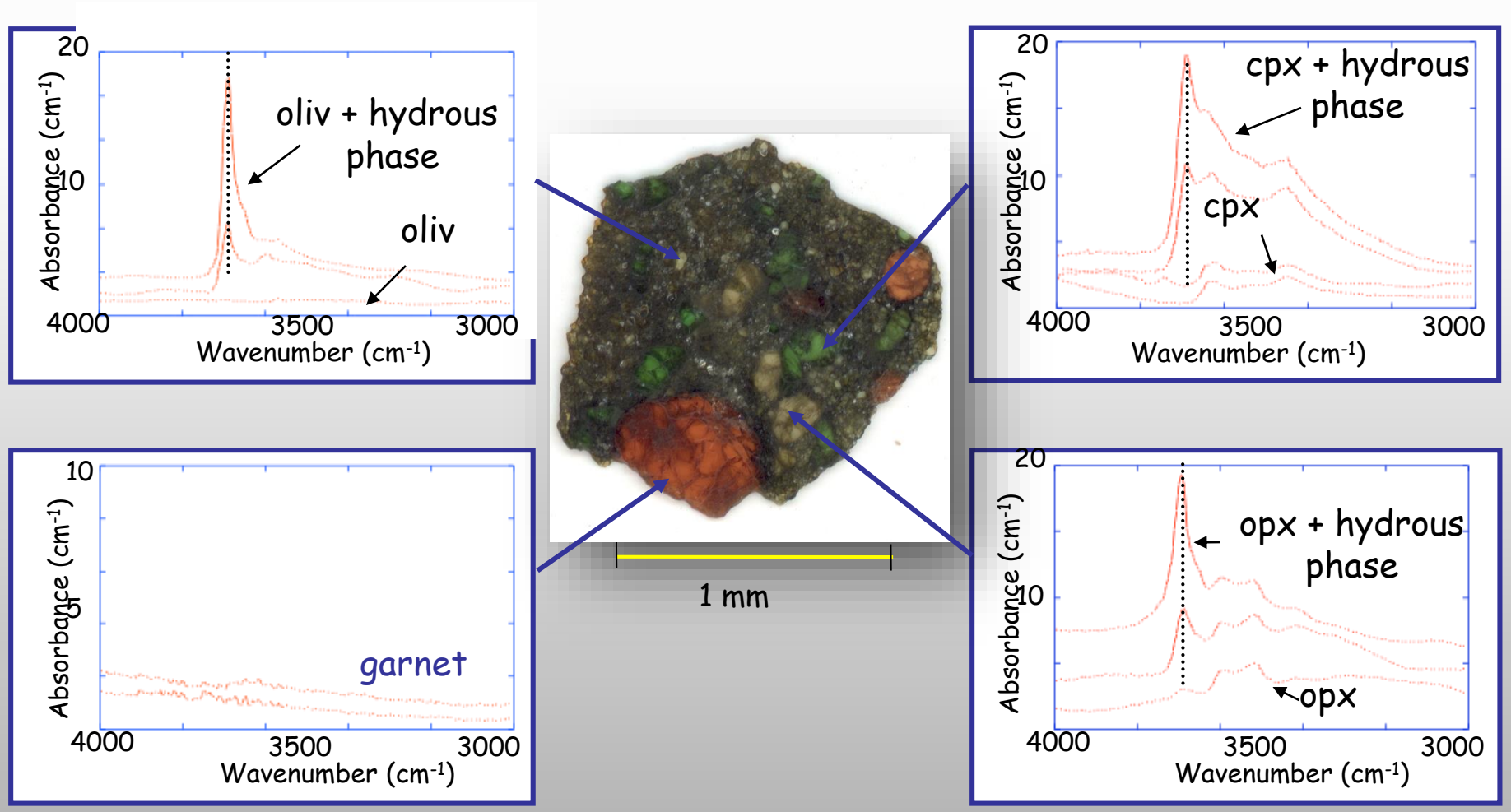

532nm, 633 nm, 790 nm

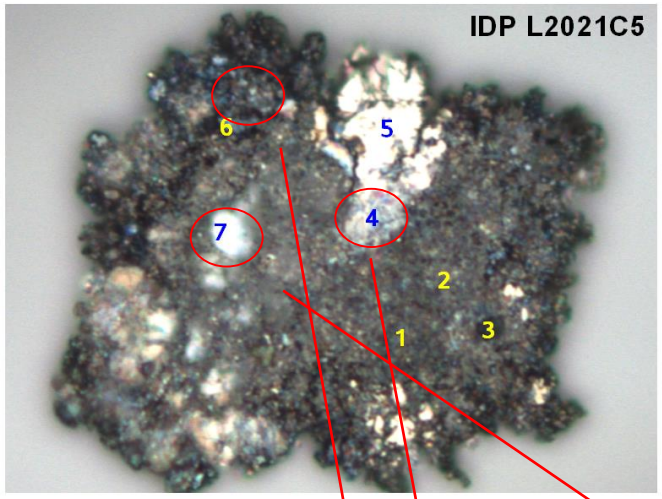

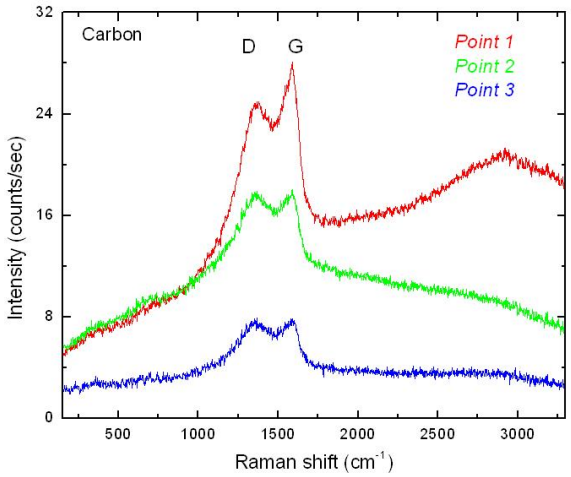

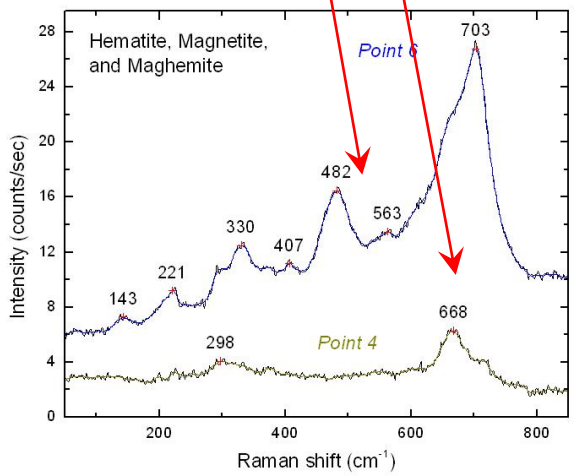

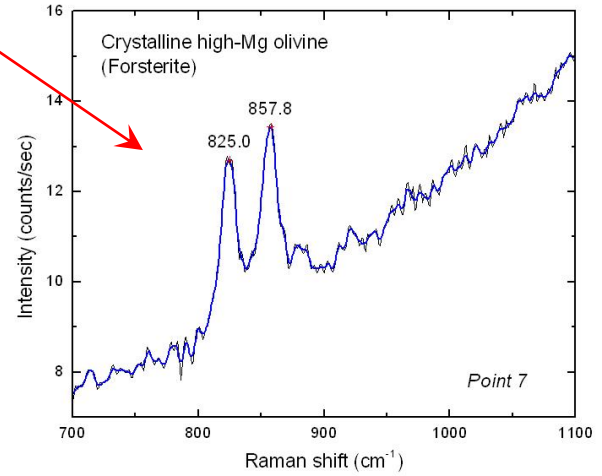

R. Rosario, J. Borg, E. Dartois, C. Sandt and P. Dumas

Abiotic synthesis of amino acids in the recesses of the oceanic lithosphere

Bénédicte Ménez, Céline Pisapia, Muriel Andreani, Frédéric Jamme, Quentin P. Vanbellingen, Alain Brunelle, Laurent Richard, Paul Dumas & Matthieu Réfrégiers

NATURE | VOL 564 | 6 DECEMBER 2018

Abiotic hydrocarbons and carboxylic acids are known to be formed on Earth, notably during the hydrothermal alteration of mantle rocks. Although the abiotic formation of amino acids has been predicted both from experimental studies and thermodynamic calculations, its occurrence has not been demonstrated in terrestrial settings. Here, using a multimodal approach that combines high-resolution imaging techniques, we obtain evidence for the occurrence of aromatic amino acids formed abiotically and subsequently preserved at depth beneath the Atlantis Massif (Mid-Atlantic Ridge).

Abiotic synthesis of organic compounds by the reduction of inorganic carbon species is thermodynamically favoured by the production of molecular hydrogen (H2), which accompanies serpentinization reactions.
The production of H2 results from the reduction of water coupled to the oxidation of ferrous iron in olivine and pyroxene, the major rockforming minerals of the upper mantle

Therefore, hydrothermal areas where active serpentinization occurs are increasingly regarded as possible settings for the appearance of the first building blocks of life and the emergence of primordial metabolisms

Our study has focused on a deeply serpentinized harzburgite that was recovered by drilling in the Atlantis Massif at a depth of 173.15 m below sea floor during the Integrated Ocean Drilling Program (IODP) Expedition 304 at Hole U1309D

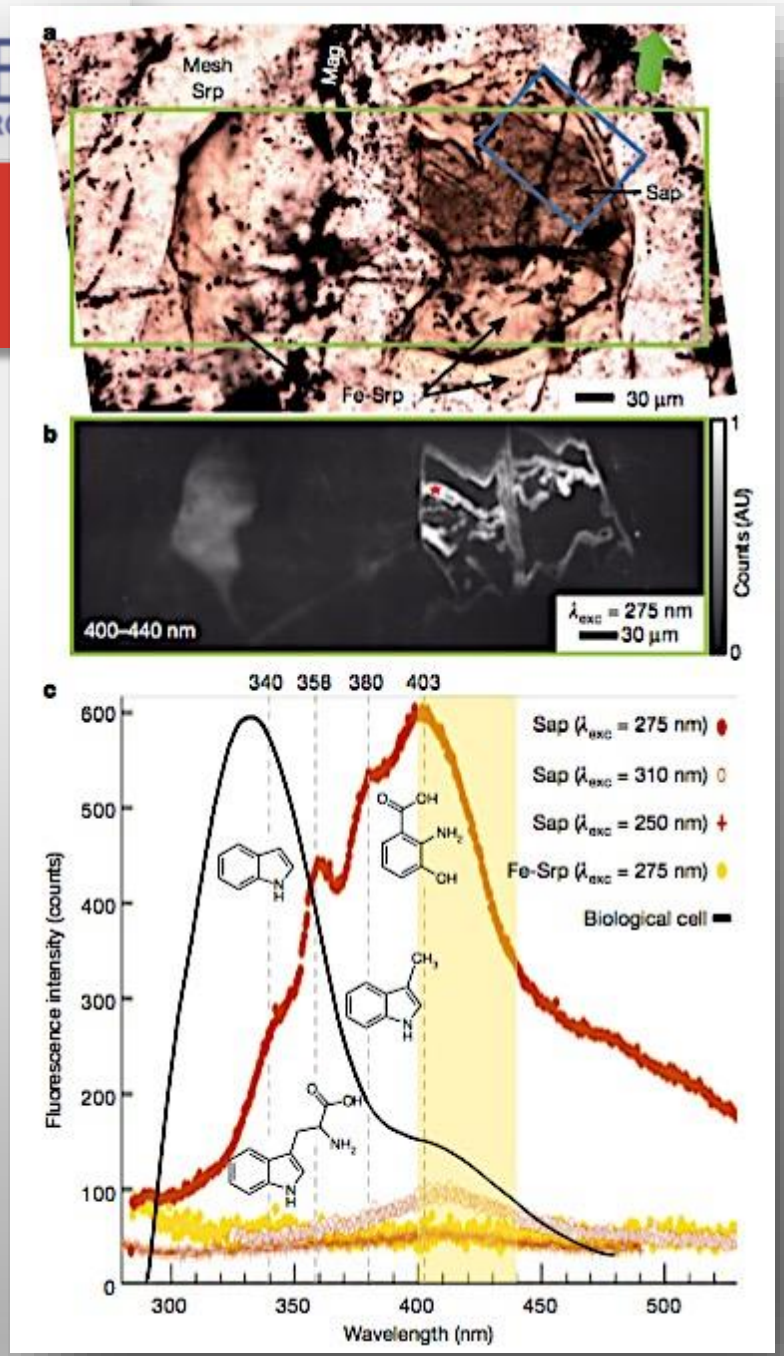

Yellow to brownish phases are frequently found in the core of the mesh serpentine (Fig. 1a). These phases correspond to Fe-rich serpentine and Fe-rich saponite enriched in organic carbon

Fig. 1 | Endogenous UV-autofluorescence locally revealed by S-DUV imaging of a highly altered mantle-rock recovered at 173.15 m below sea floor from IODP Expedition 304 Hole U1309D. UV-fluorescence emerged from heteroatomic aromatic compounds shown to be spatially restricted to an Fe-rich clay in which they are heterogeneously distributed. **a**, Optical image showing yellow to brownish phases identified as Fe-rich serpentine (Fe-Srp) and Fe-rich saponite (Sap), hosted in a serpentinized harzburgite with olivine being replaced by magnetite (Mag) and serpentine exhibiting a characteristic mesh texture (mesh Srp); the green arrow indicates sample orientation. **b**, Full field S-DUV image of the area depicted by the light-green rectangle in **a**, collected between 400 and 440 nm using excitation (λ_{exc}) at 275 nm. AU, arbitrary units. **c**, Fluorescence emission spectra collected with excitation wavelengths of 250, 275 and 310 nm at the location shown by an asterisk in **b**. The spectra collected at 250 and 310 nm do not show a notable UV-autofluorescence signal, whereas the spectrum at 275 nm displays fluorescence characteristic of indole at 340 ± 6 nm, tryptophan at 358 ± 3 nm, skatole at 380 ± 3 nm, and hydroxyanthranilic acid at 403 ± 3 nm[18] (mean ± s.d. of three independent fits performed on three areas). Also shown are a fluorescence emission spectrum collected at 275 nm in the Fe-rich serpentine and the typical emission spectrum of a biological cell showing maximum fluorescence emission, mainly arising from protein-forming tryptophan, shifted to 335 nm[21]. The orange area in **c** represents the fluorescence detection range used in **b**. The blue box in **a** indicates the location of complementary S-FTIR measurements (Extended Data Fig. 3).

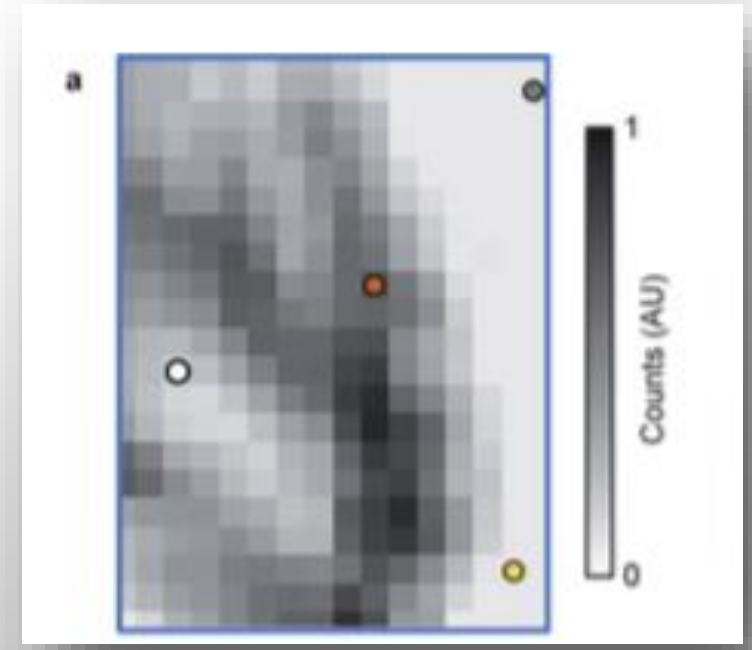

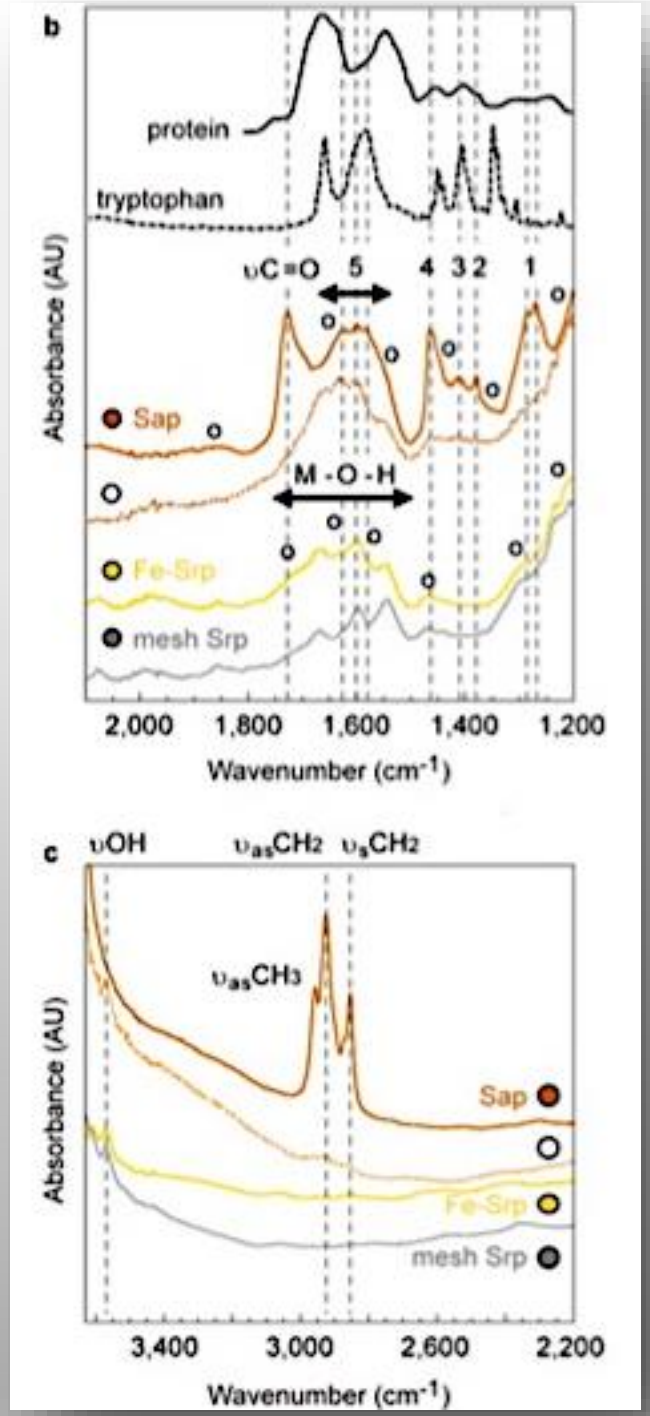

Extended Data Fig. 3 | S-FTIR confirmed the presence of N-bearing organic compounds in the Fe-rich saponite. a, S-FTIR distribution maps of the aliphatic CH_2/CH_3 stretching band area between 2,800 and 3,000 cm^{-1} shown in **c** and collected in the area indicated by the blue box in Fig. 1a. **b**, **c**, Associated S-FTIR spectra. The spectrum collected in the C-rich saponite (Extended Data Fig. 2a, b) shows the presence of organic compounds with modes at (1) 1,270 cm^{-1} and 1,285 cm^{-1}, (2) 1,380 cm^{-1}, (3) 1,412 cm^{-1}, (4) 1,460–1,465 cm^{-1}, (5) 1,550–1,650 cm^{-1}, and 1,728 cm^{-1} in **b**, and 2,855, 2,871, 2,924 and 2,958 cm^{-1} in **c**. Band assignments are compiled in Supplementary Table 3. Contributions of the H–O–H bending from the saponite interlayer water at 1,627 cm^{-1} may interfere[15]. Also shown are the S-FTIR spectra collected in the mesh serpentine and the Fe-rich serpentine, both being nearly depleted in absorption bands related to organic compounds. They show instead characteristic O–H stretching bands at 3,570 and 3,610 cm^{-1} and M–O–H bending modes (with M indicating any of the cations in the hydrated silicate structure) in the range 1,500–1,680 cm^{-1}. Dotted brown curves correspond to a mixture of saponite and serpentine. Precise locations of analysis are indicated in **a** with the corresponding coloured dots. FTIR spectra of protein[26] and L-tryptophan (https://webbook.nist.gov/cgi/cbook.cgi?ID=C73223&Mask=80) are shown for comparison. 'υ' denotes overtone-combination bands; 'ν' denotes stretching; 'ν_{as}' and 'ν_s' denote asymmetric and symmetric stretching, respectively.

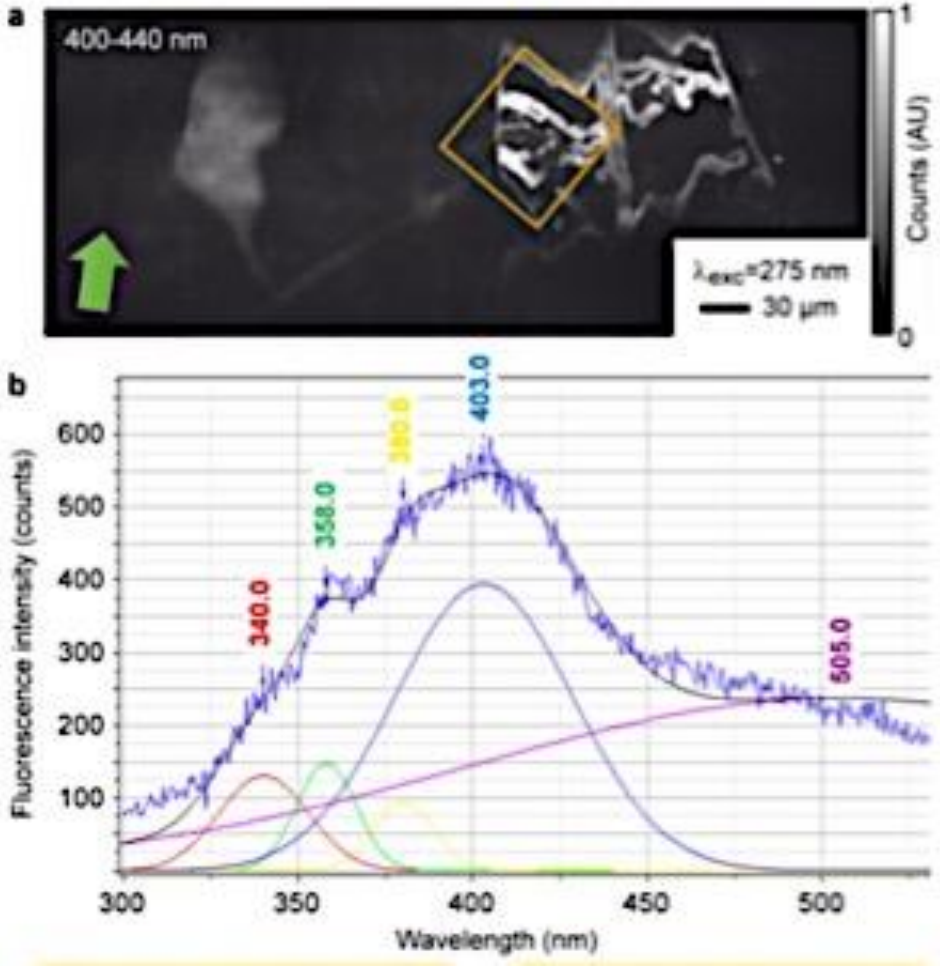

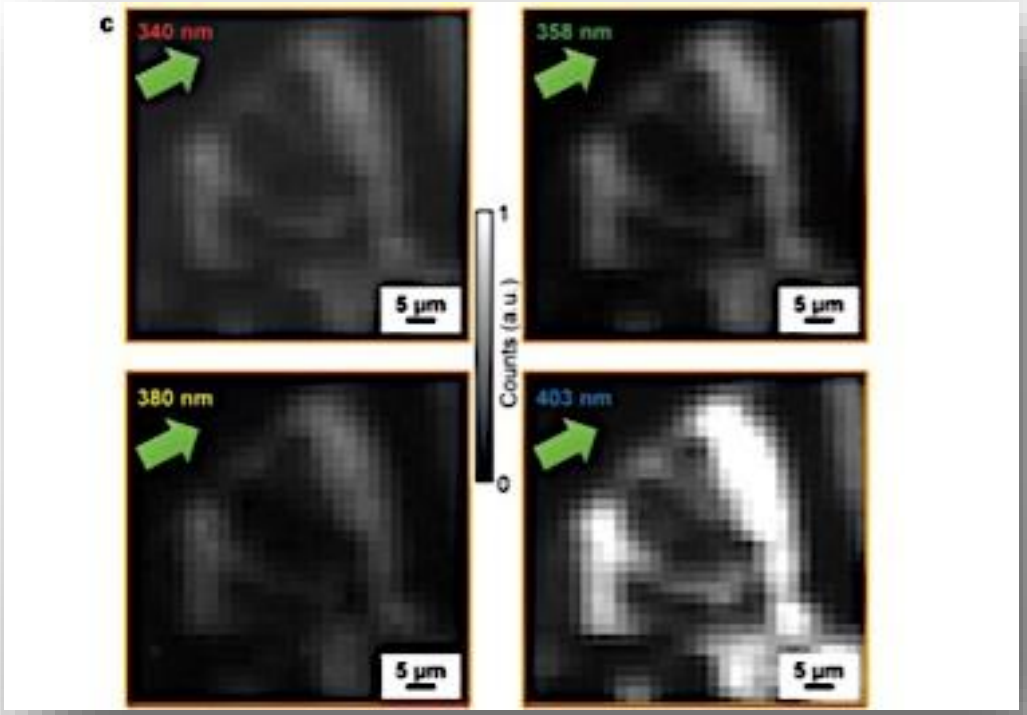

Extended Data Fig. 5 | S-DUV spectral signature of the endogenous fluorescence revealed in the Fe-rich saponite. a, Full-field S-DUV image displayed in Fig. 1 and collected using an excitation wavelength (λ_{exc}) of 275 nm, and a detection range of fluorescence emission between 400 and 440 nm. **b**, Fluorescence emission spectra collected with excitation wavelength of 275 nm summed from the hyperspectral datacube acquired in the area indicated by the orange box in **a** (30 s per point, 2-µm step). Fit of the S-DUV hyperspectral maps, performed using Gaussian functions and 10 iterations, resolved 4 main contributions at 340 ± 6, 358 ± 3, 380 ± 3 and 403 ± 3 nm (mean ± s.d. of three independent measurements). **c**, Associated spatial distributions of fluorescence emissions at 340, 358, 380 and 403 nm. They revealed systematic co-localization of these four components. The green arrows indicate sample orientation.

The results reported here clearly indicate that the clay-forming hydrothermal alteration of oceanic rocks has a fundamental role in the synthesis and stabilization of complex organic compounds such as aromatic amino acids. This may have far-reaching implications for the carbon and nitrogen cycles in the Earth's system, as well as for the potential for prebiotic chemistry on Earth and the deep biosphere.

Conclusions

- **Infrarouge et Raman, les deux méthodes de spectroscopie vibrationnelle sont d'un grand apport en science de la terre.**

- **Leur complémentarité est essentielle à la détermination des phases présentes, leur inclusions**

- **La fluorescence est très performante pour identifier de faible quantité de matière.**

- **Les combinaisons de ces trois approches sont évidentes et souhaitable**

Conclusions

- **- La microscopie permet, dans chaque cas d'atteindre des résolution de l'ordre de quelques microns, microns voire moins.**

- **L'utilisation de source telle que synchrotron apporte beaucoup aux performances de ces instruments.**

- **A sein d'un synchrotron comme SOLEIL, et à défaut de présence de ces trois moyens expérimentaux dans votre laboratoires des projets de recherche peuvent être soumis pour être réalisés au centre de rayonnement synchrotron SOLEIL.**